Validation Effort of LAVA Parachute Simulation Capability with ASPIRE Flight Data

Jonathan Boustani, Francois Cadieux, Gaetan K. Kenway

Michael F. Barad, Cetin C. Kiris

Computational Aerosciences Branch, NASA Ames Research Center, Moffett Field, CA, 94035, USA

Parachute FSI Workshop

Monday, January 31st, 2022

POC: cetin.c.kiris@nasa.gov

Outline

- ❑ Motivation
  - Overview, problem description
- ❑ Approach
  - Immersed boundary method (CFD)
  - Nonlinear structural dynamics solver (CSD)
- ❑ Enhancements and Grid Sensitivity Studies
  - Code optimization for large-scale FSI
  - Modeling broadcloth porosity
  - Contact identification and enforcement
  - Grid resolution studies (capsule wake, static canopy)
- ❑ ASPIRE FSI Simulations
- ❑ Summary

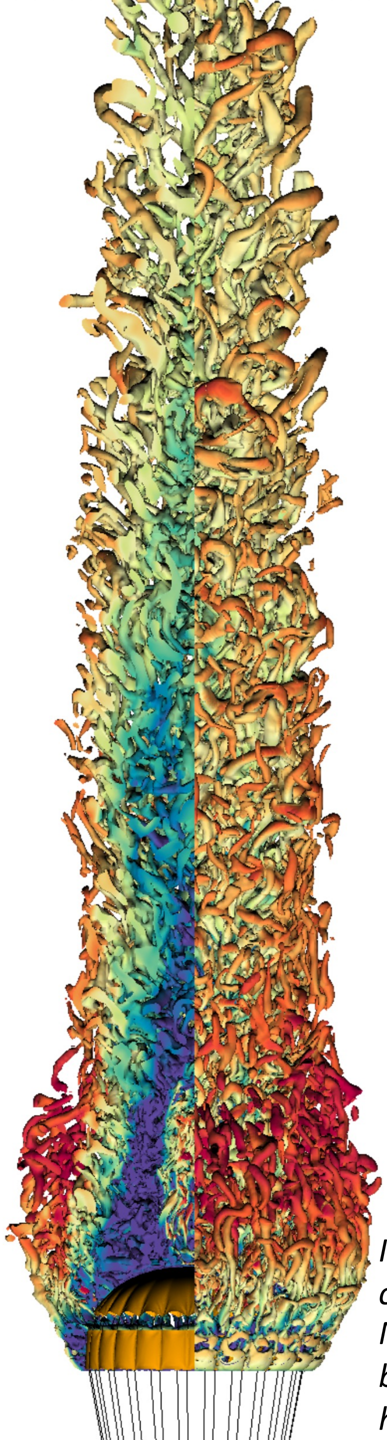

Isocontours of Q-criterion colored by Mach number where blue is lower and red is higher.

Motivation

- In FY21, ESM tasked the LAVA team with demonstrating the capability to simulate the supersonic parachutes used in the Mars entry process

- Following the low-density supersonic decelerator (LDSD) missions, the agency concluded that its ability to model and predict the stresses during inflation are lacking

- The ASPIRE missions were conducted to develop the capability to test parachutes in high-altitude, supersonic conditions and, in light of LDSD, to reduce risk ahead of Mars 2020

(NASA/JPL)

LAVA's Adaptive Cartesian Navier-Stokes Solver

- ❑ Using an immersed boundary method allows automatic volume mesh generation for arbitrarily complex geometries

- ❑ Arbitrary motion and deformation of a Lagrangian geometry is easily tracked over a static Eulerian `background' mesh

- ❑ Higher-order accurate
  - $5^{th}/6^{th}$-order accurate WENO

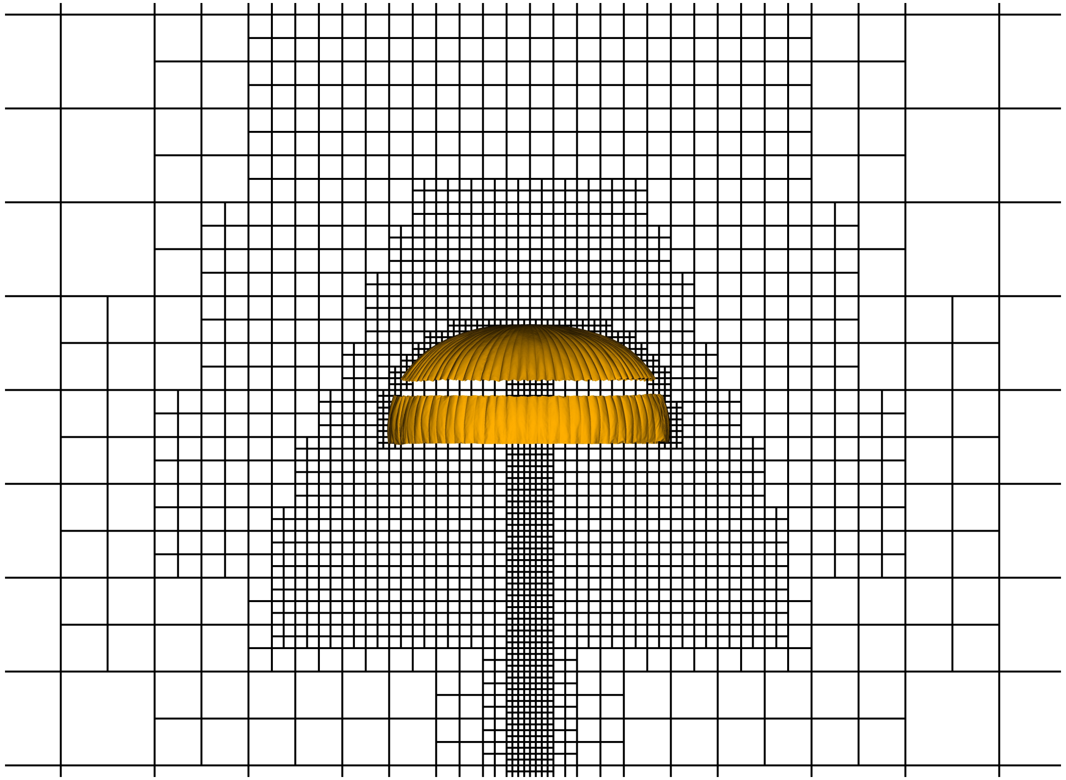

Slice of a general Cartesian block structure around an inflated parachute geometry. Each block represents 16x16x16 grid points.

Nonlinear Structural Dynamics Solver

- The LAVA-Structural solver is capable of linear and nonlinear steady, unsteady, and modal analysis

- Elements available:
  - Bernoulli-Euler beam
  - Constant strain triangular shell
  - Cable
  - **MITC3 triangular shell**
  - **Timoshenko beam**

- Time integrators:
  - Implicit Newmark-β
  - **Explicit central difference**
  - Explicit Noh-Bathe

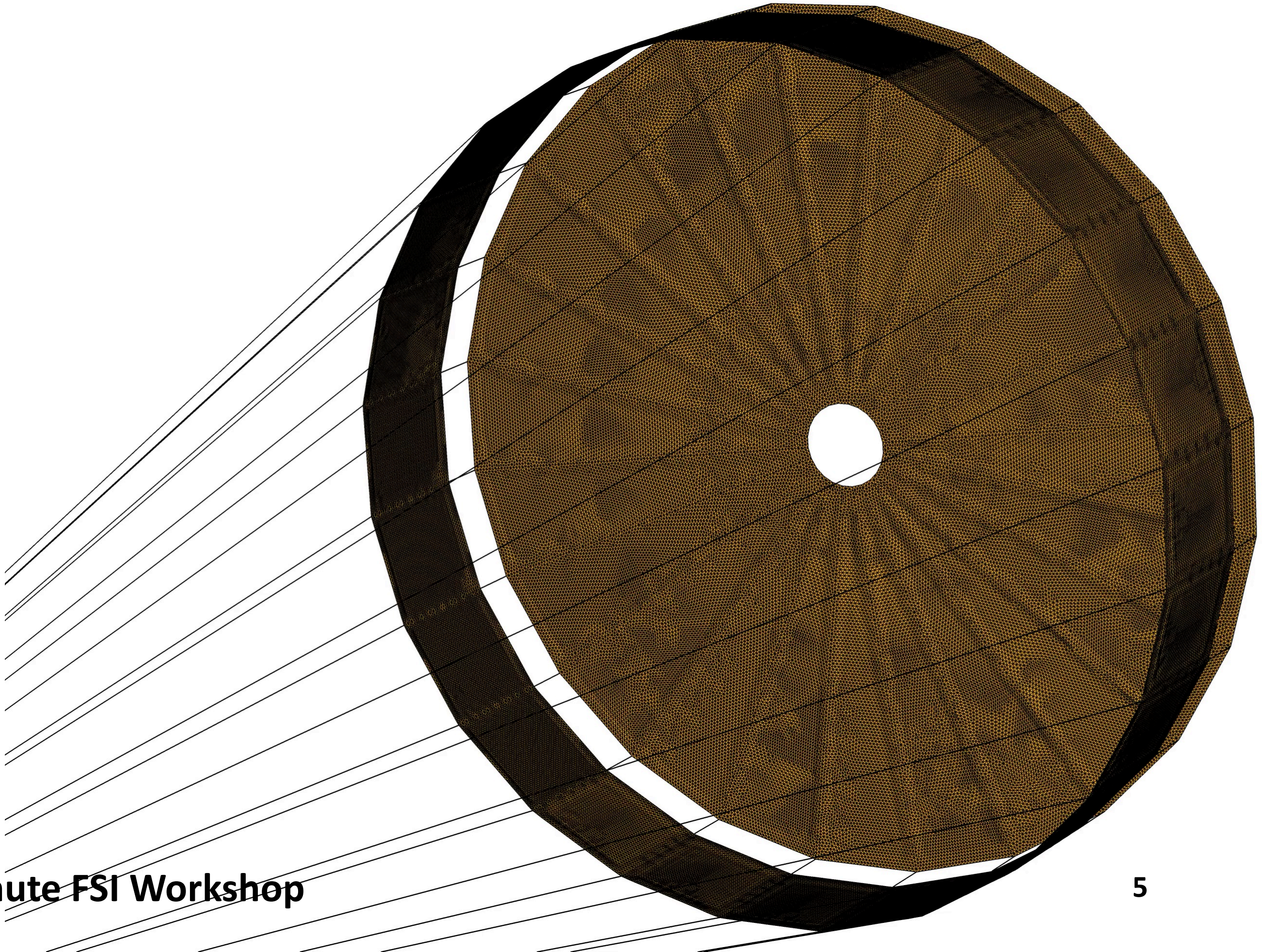

Launch, Ascent, and Vehicle Aerodynamics (LAVA) Framework

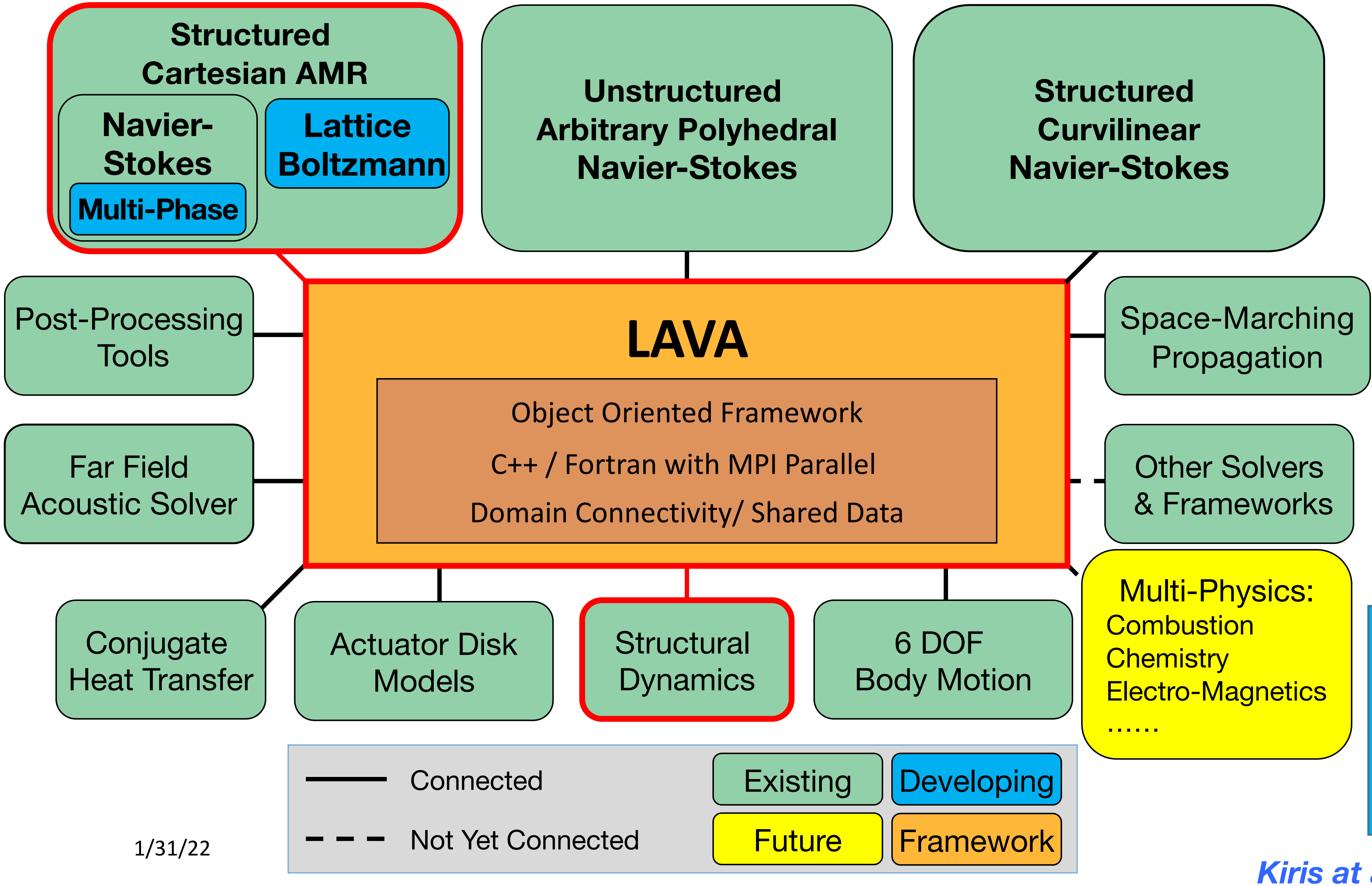

Other Development Efforts

- Higher order and low dissipation
- Curvilinear grid generation
- Wall modeling
- LES/DES/ILES Turbulence
- HEC (optimizations, accelerators, etc)

Kiris at al. AIAA-2014-0070 & AST-2016

Optimizations for Large-Scale FSI

- The CSD solver starts the FSI simulation in a semi-folded shape →
  - Resolving each of the 80 gores may take millions of DOF
- Moving to such large-scale simulations motivates the use of an explicit solver
  - More readily parallelizable than a direct solver and requires less memory
  - Due to such a small thickness, a direct solver may also struggle to converge at times
  - For these reasons, the central difference method was implemented

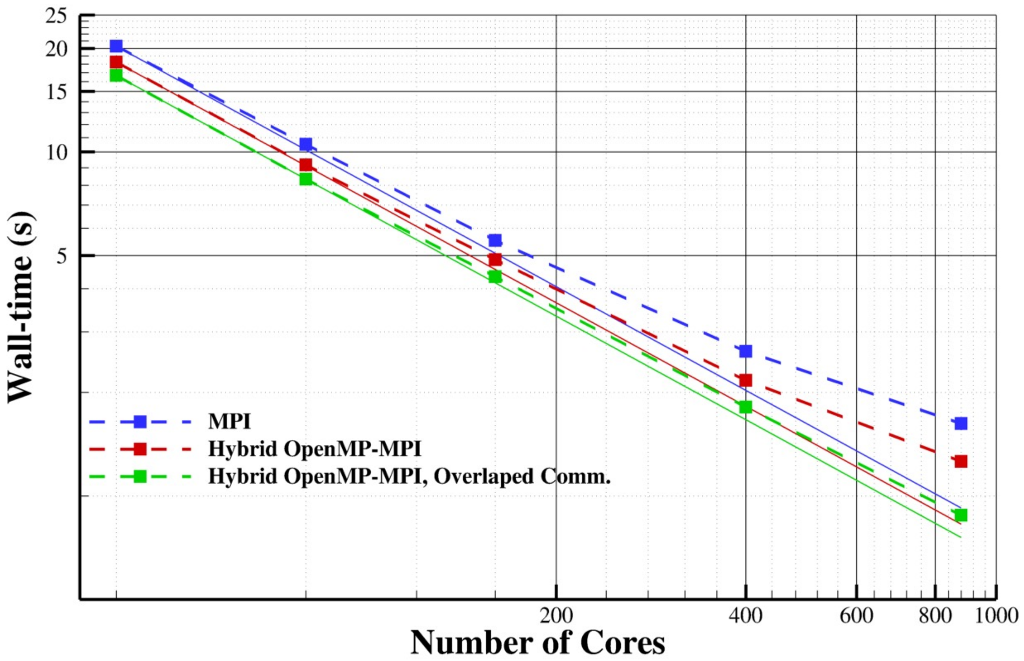

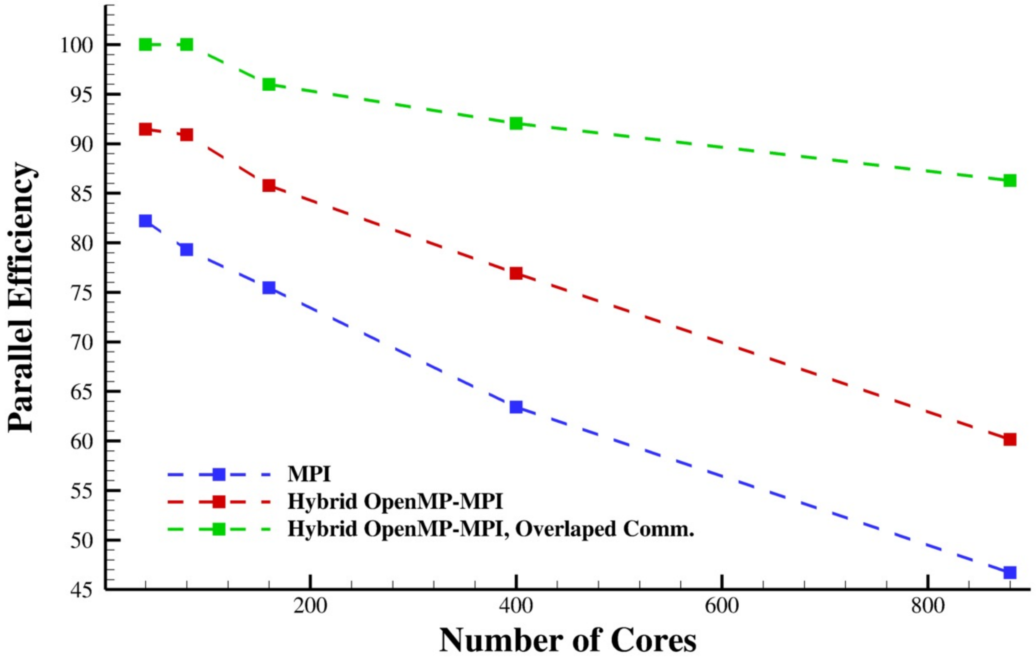

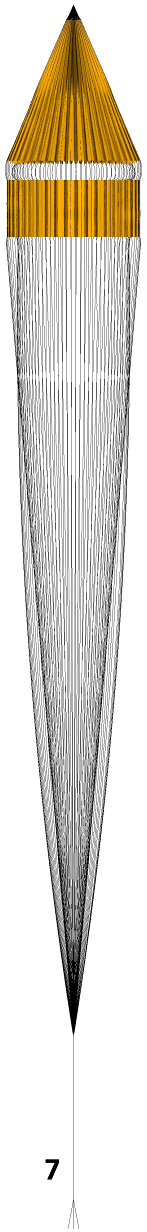

Modeling Broadcloth Porosity

- A closed-form solution to the Darcy-Forchheimer momentum equation is obtained and implemented as a jump condition
  - The jump conditions prevents the need to spatially resolve the thickness of the parachute like typical source term models would

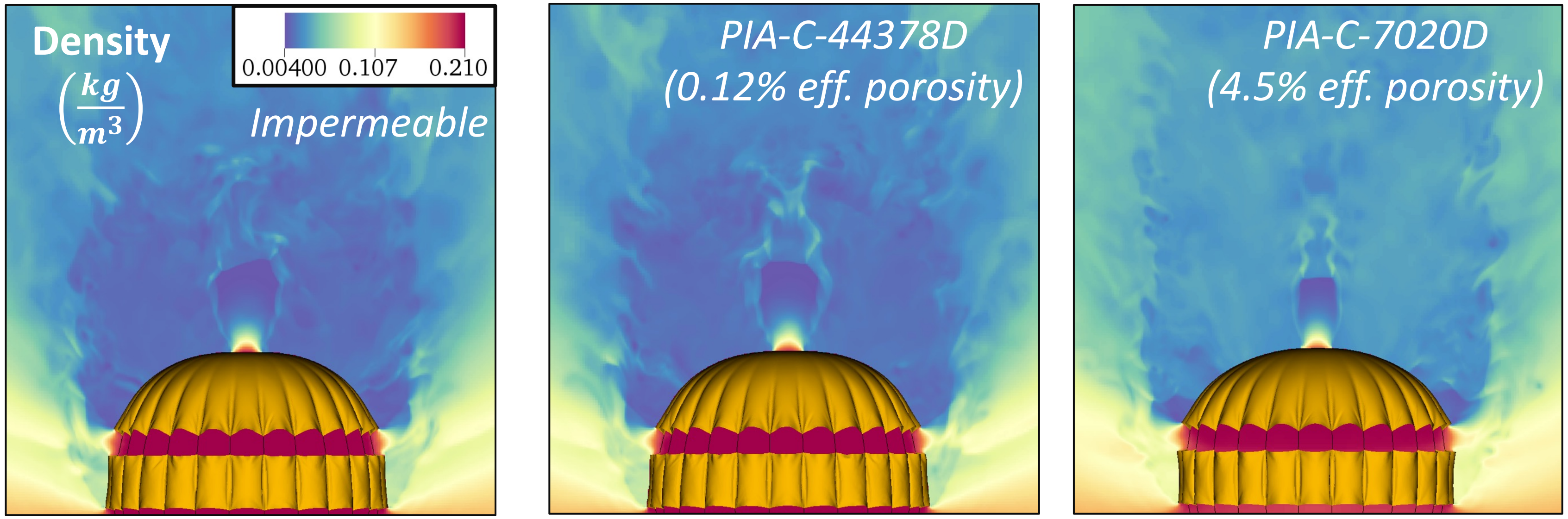

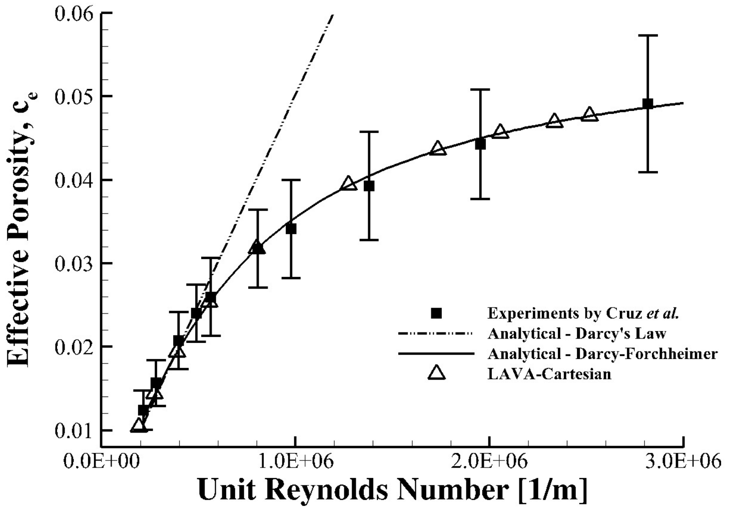

Comparison of results from experiments by Cruz et al. and simulations by LAVA-Cartesian for PIA-C-7020D Type I broadcloth.

- The lack of a strong recirculation region behind the PIA-C-7020D canopy and high-density fluid simply passing though the canopy raises the density in the wake of the PIA-C-70270D canopy
  - Lower drag forces can be expected

Contact Identification and Enforcement

- A contact identification algorithm based on optimized ray-tracing libraries was developed
  - Contact is identified between two faces when a ray extending normal to one of the faces intersects the other face within a set distance relative to the CFD grid spacing

- Enforcement is conducted via a physics-based model for simulating contact mechanics between the two faces
  - A penalty contact impulse is derived from first principles to model the exchange of momentum required to enforce an elastic collision

Setup and results from a canonical 1D contact problem

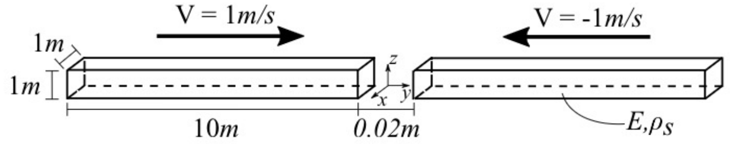

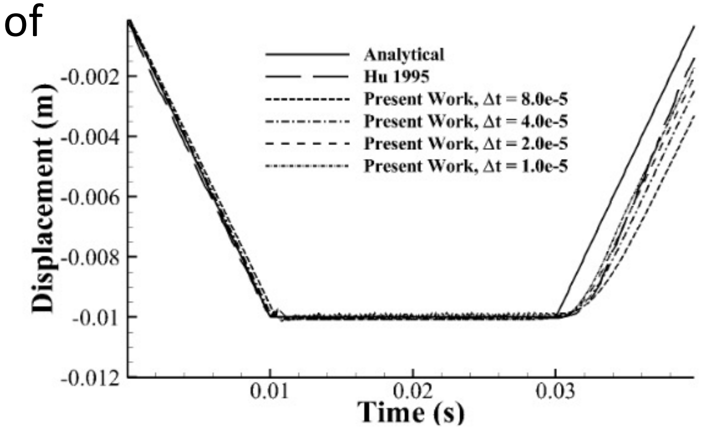

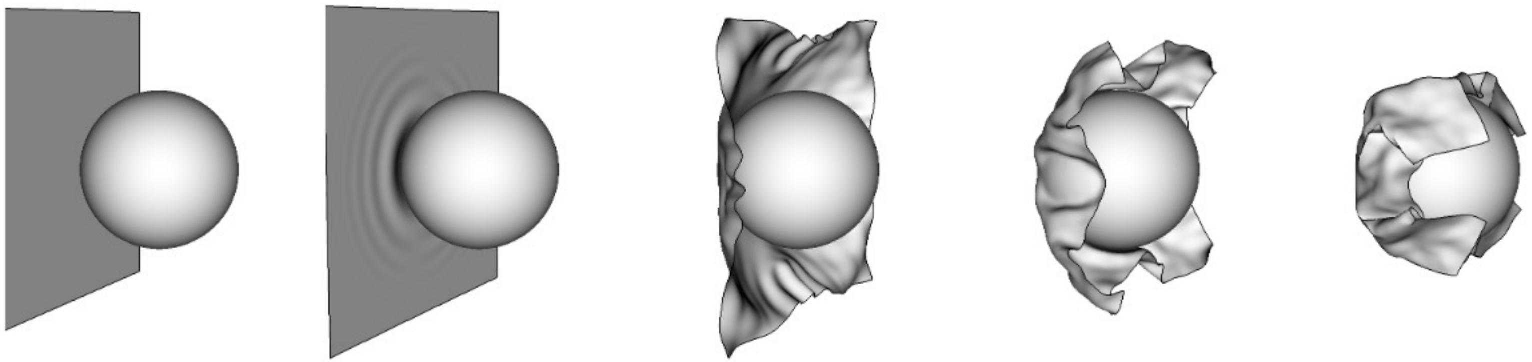

Snapshots in time of a test case demonstrating the contact identification and enforcement method

Contact Identification and Enforcement

- A contact identification algorithm based on optimized ray-tracing libraries was developed
  - Contact is identified between two faces when a ray extending normal to one of the faces intersects the other face within a set distance relative to the CFD grid spacing

- Enforcement is conducted via a physics-based model for simulating contact mechanics between the two faces
  - A penalty contact impulse is derived from first principles to model the exchange of momentum required to enforce an elastic collision

<u>Simulation Statistics:</u>
- ~0.15s per timestep, including contact detection
- 500k total timesteps, ~0.2s of simulation time
- $\Delta t_{crit.}$ ranged from 7E-7s to 1.7E-6s during inflation
- 560 cores used, ~2.5k DOF/core
- Cores spread across 20 Broadwell nodes

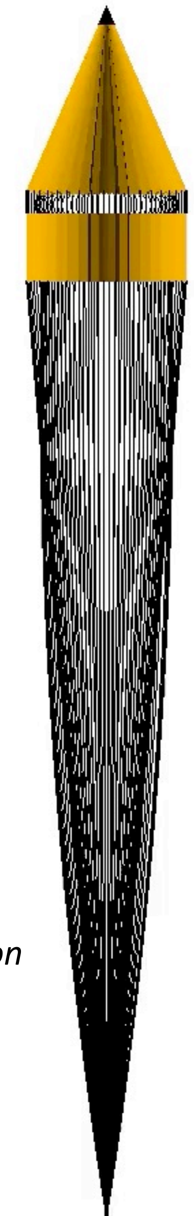

Inflating parachute from a CSD-only simulation evaluating the contact identification and enforcement algorithm. The CSD solver is exposed to a 474Pa surface normal force.

Grid Resolution Study: Slender Capsule Wake

- ASPIRE saw the use of a slender capsule as opposed to typical bluff-bodied entry capsules
  - This significantly affects the wake deficit and the level of capsule wake/canopy bow shock interaction

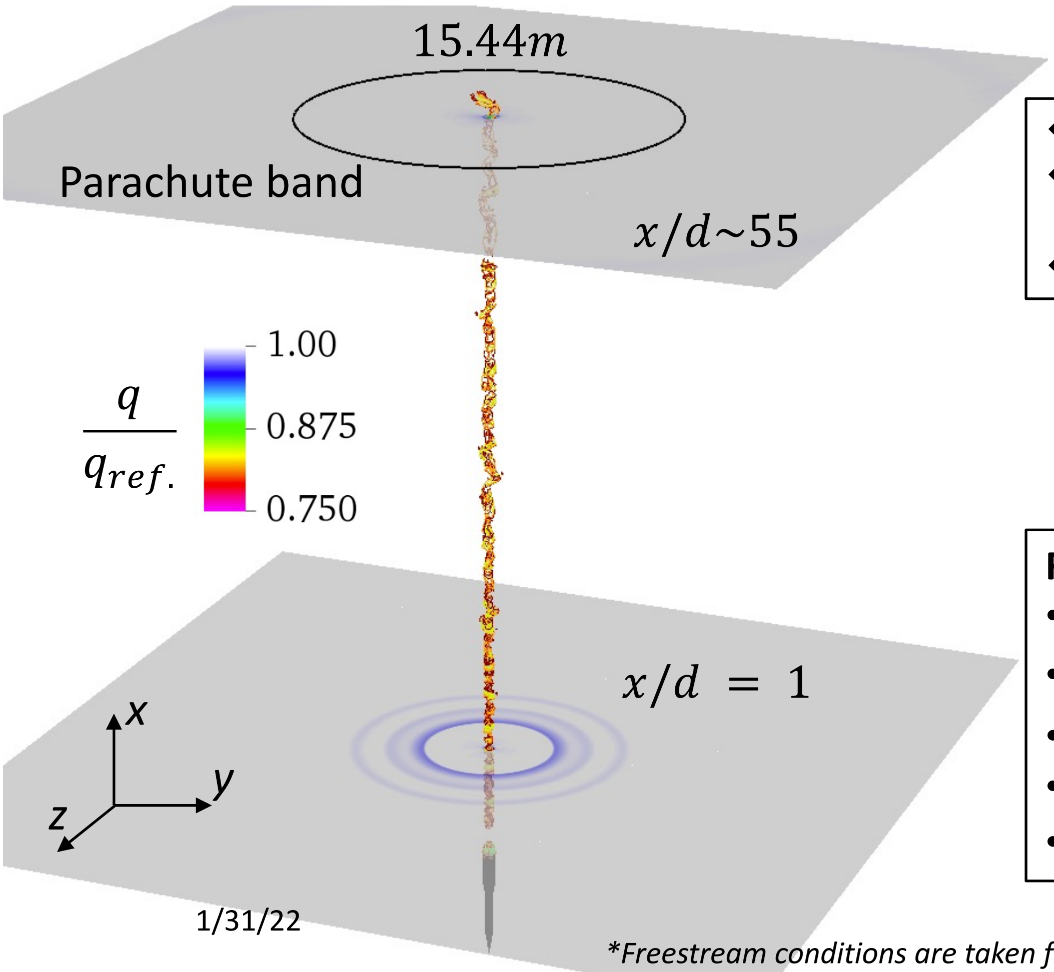

- Probes at: $y = 0.5d, y = d, y = 2d$
- Trailing distance of: $x = 40m$ behind the capsule nose
- Capsule diameter: $d \sim 0.72m$

Freestream conditions*

- $P = 251.45Pa$
- $U = 558.2\frac{m}{s}$
- $T = 253.215K$
- $q_{ref} = 538Pa$
- $M = 1.75$

- A previous study by Muppidi *et al.* on the ASPIRE capsule found that the wake deficit quickly returns to unity as the probes move radially outward

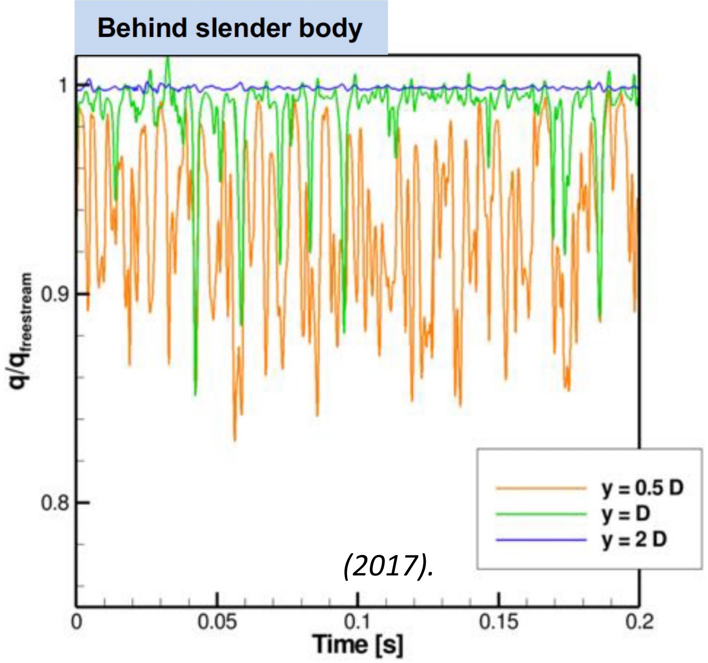

Image adjusted from Muppidi et al. 38th IEEE Aerospace Conference (2017).

Freestream conditions are taken from Muppidi et al. 38th IEEE Aerospace Conference (2017)

Grid Resolution Study: Slender Capsule Wake

- In order to determine the level of grid resolution required to capture the slender wake, a grid resolution study is performed

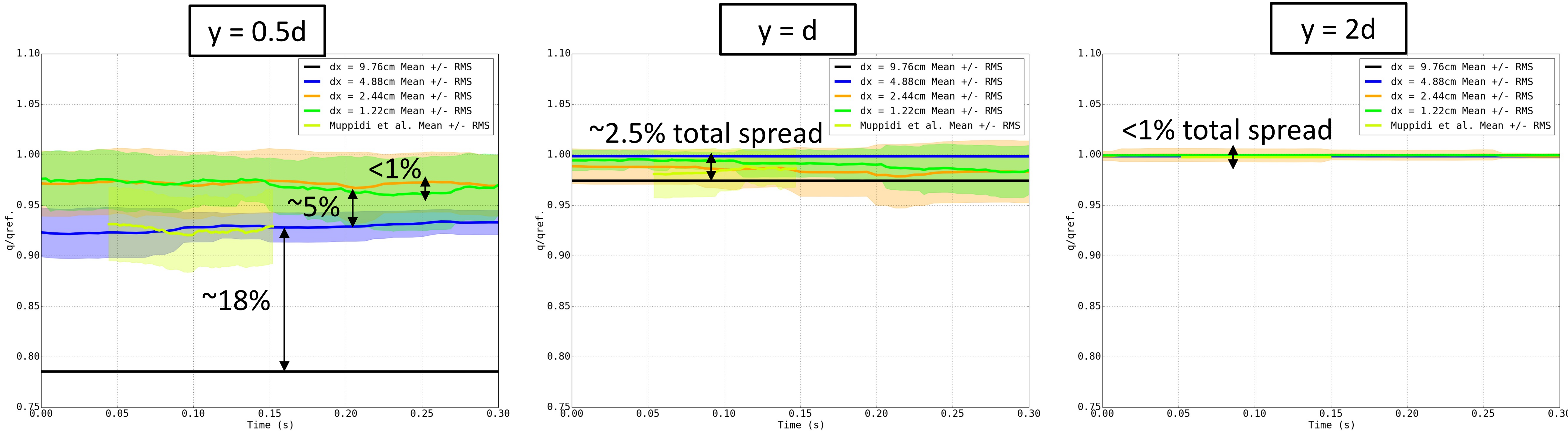

- The solutions converge quickly with successive halving of the volume grid spacing
  - Between the 2.44cm and 1.22cm resolutions, the wake deficit changes less than 1% at all 3 probes

Grid Resolution Study: Static Canopy

- The same analysis is performed for the static, inflated canopy
  - The 3 grids are scaled by factors of $2^{\frac{1}{3}}$ such that the number of grid points approximately doubles/halves

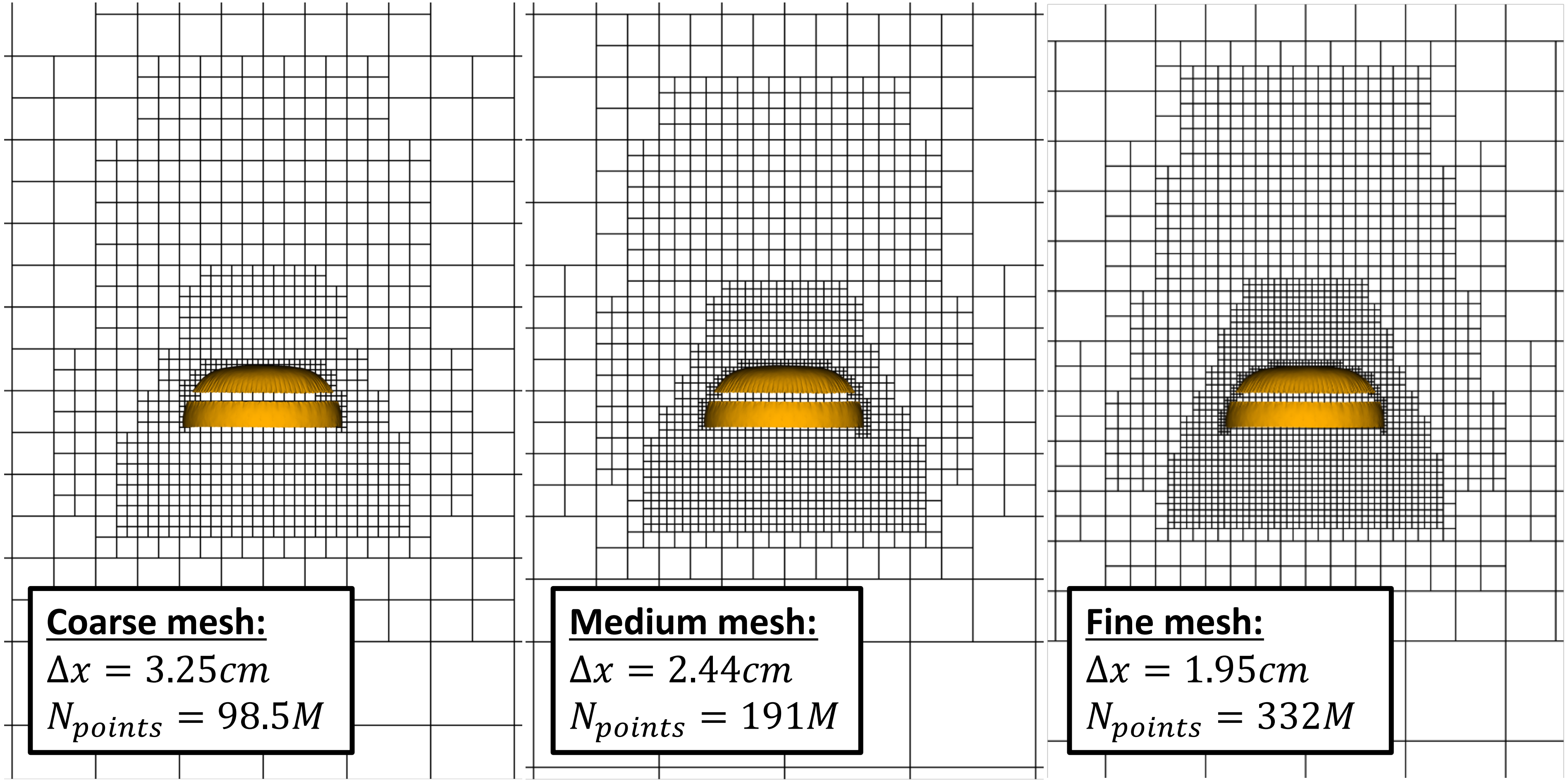

Freestream conditions*

- $P = 219.22Pa$
- $U = 567.74\frac{m}{s}$
- $T = 249.339K$
- $q_{ref} = 491.68Pa$
- $M = 1.79$

**Freestream conditions are taken at the line stretch event described by the ASPIRE SR01 post-flight test report*

Grid Resolution Study: Static Canopy

- Small sensitivity in the total drag force to the grid resolution is observed
  - Less than 1% difference between solutions in terms of aerodynamic drag
  - Qualitatively, the bow shock and wake structures are very similar between solutions

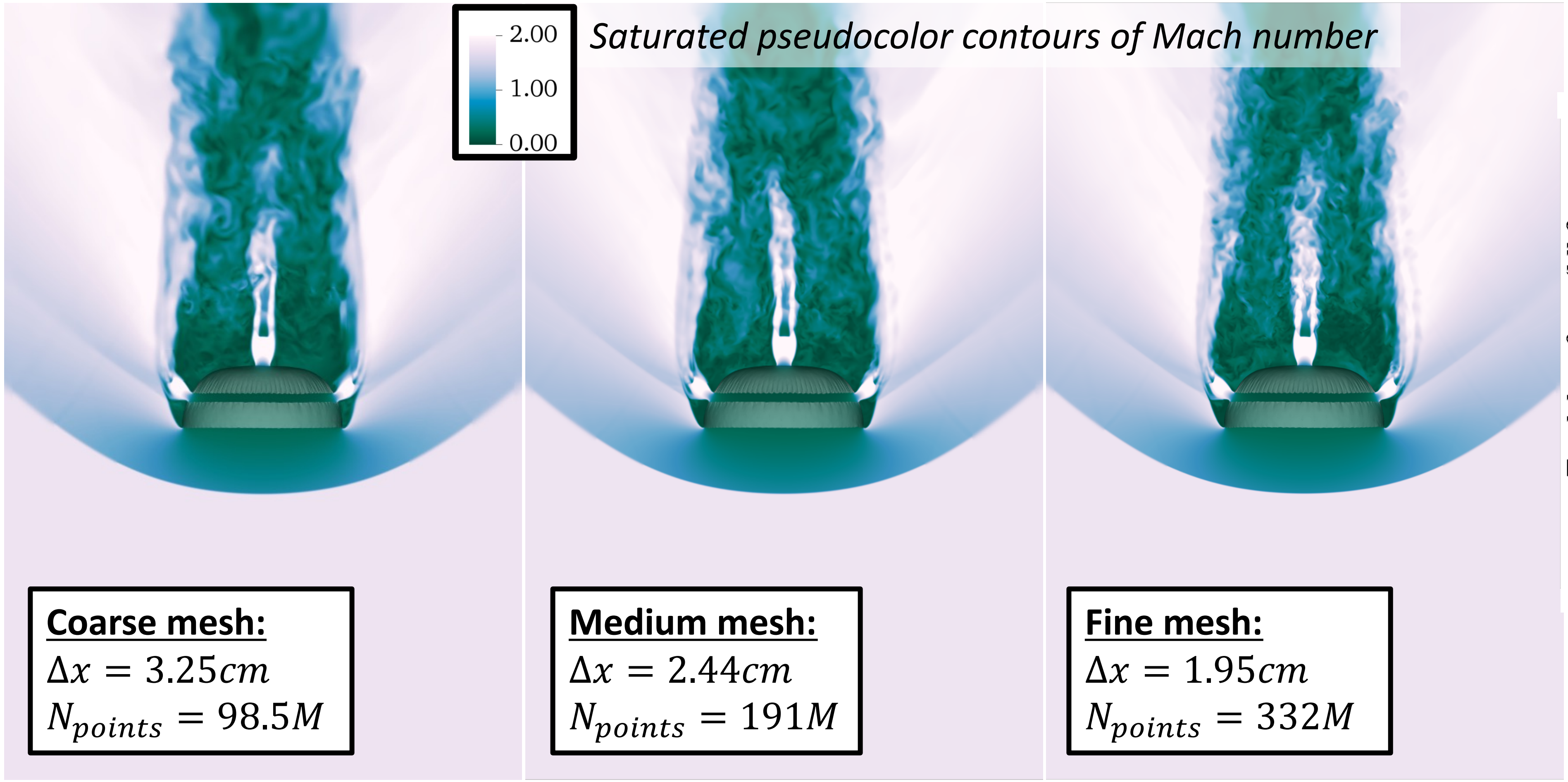

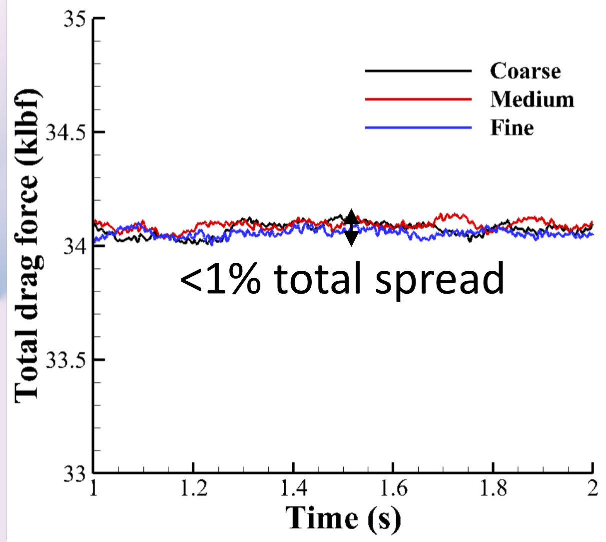

ASPIRE FSI Simulations

- ❑ Finally, the porosity and contact methods, and the results of the grid sensitivity study, are used in FSI simulations of the ASPIRE SR01 flight test

- ❑ The FSI simulation is started from a precursor CFD-only simulation

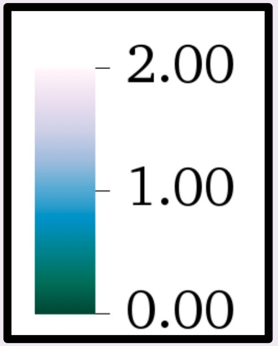

Saturated pseudocolor contours of Mach number

ASPIRE FSI Simulations

- ❑ Once the aerodynamic loads become statistically stationary, the FSI simulation is started
  - In other words, the CFD simulation is restarted, and the coupled CFD+CSD simulation begins

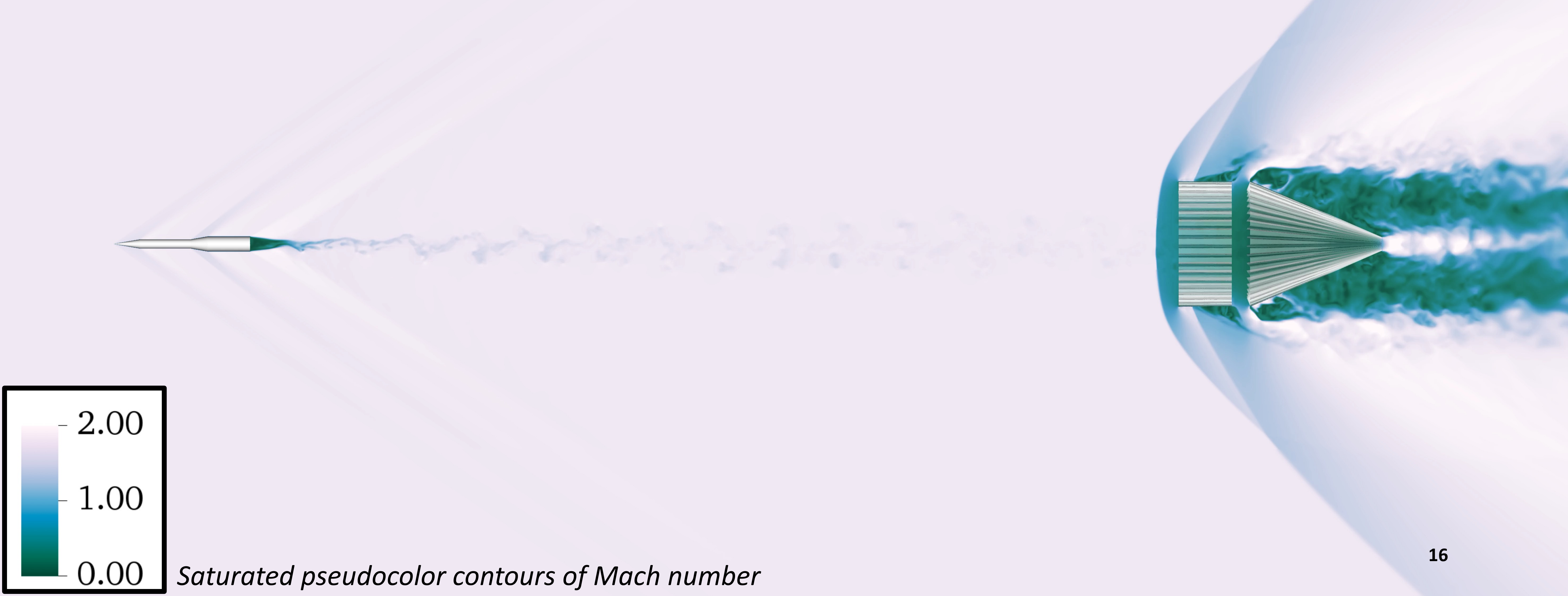

Saturated pseudocolor contours of Mach number

ASPIRE FSI Simulations

- Once the aerodynamic loads become statistically stationary, the FSI simulation is started
    - In other words, the CFD simulation is restarted, and the coupled CFD+CSD simulation begins

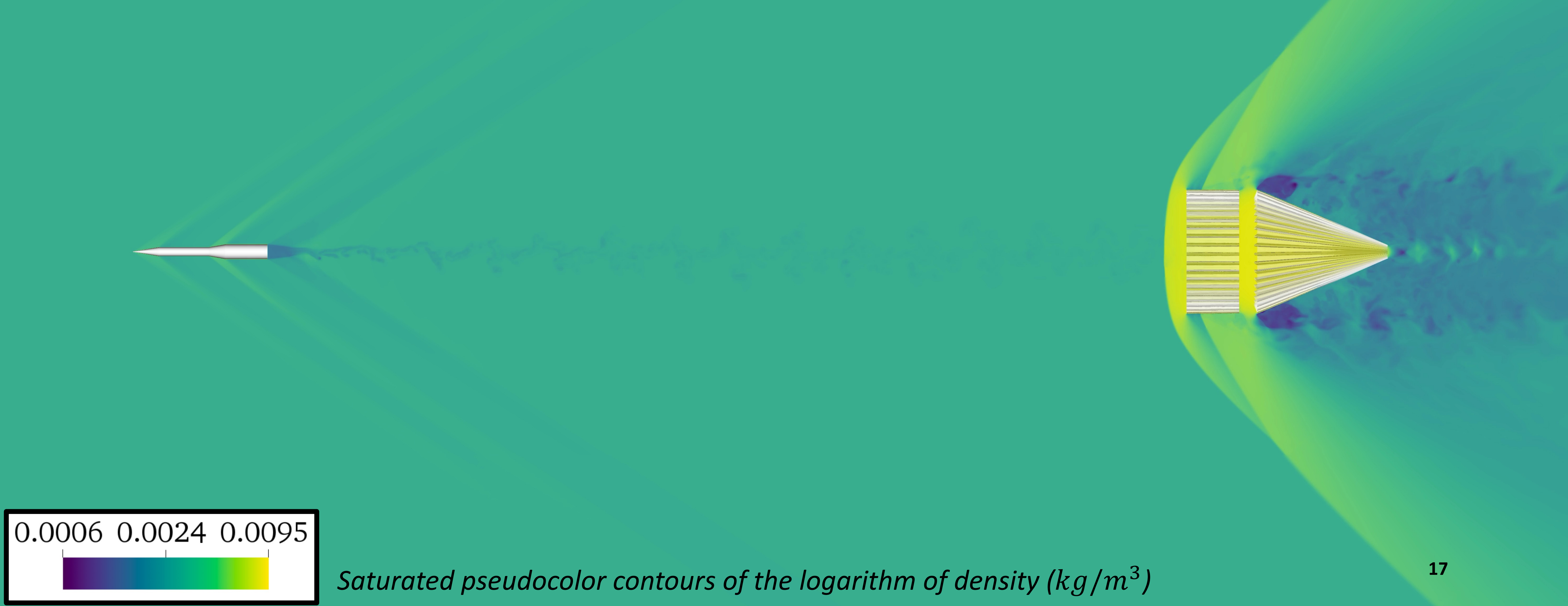

Saturated pseudocolor contours of the logarithm of density (kg/m^3)

Comparison of ASPIRE FSI Simulations with Flight Data

- The combined restoring force in the 3 beam elements at the leading edge of the triple bridle are used to measure the parachute forces
  - Similar to load pins used in flight tests

- To determine if the overshoot is from discretization error, a grid sensitivity study is performed

triple bridle

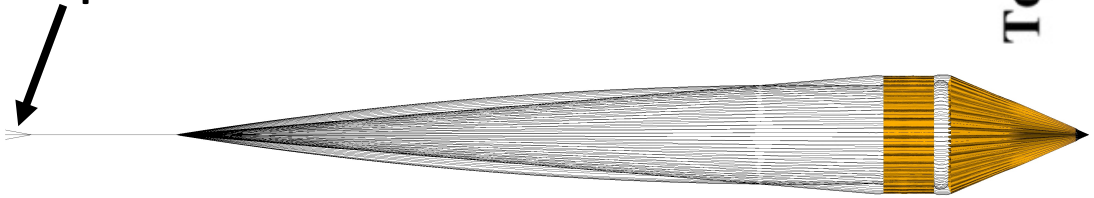

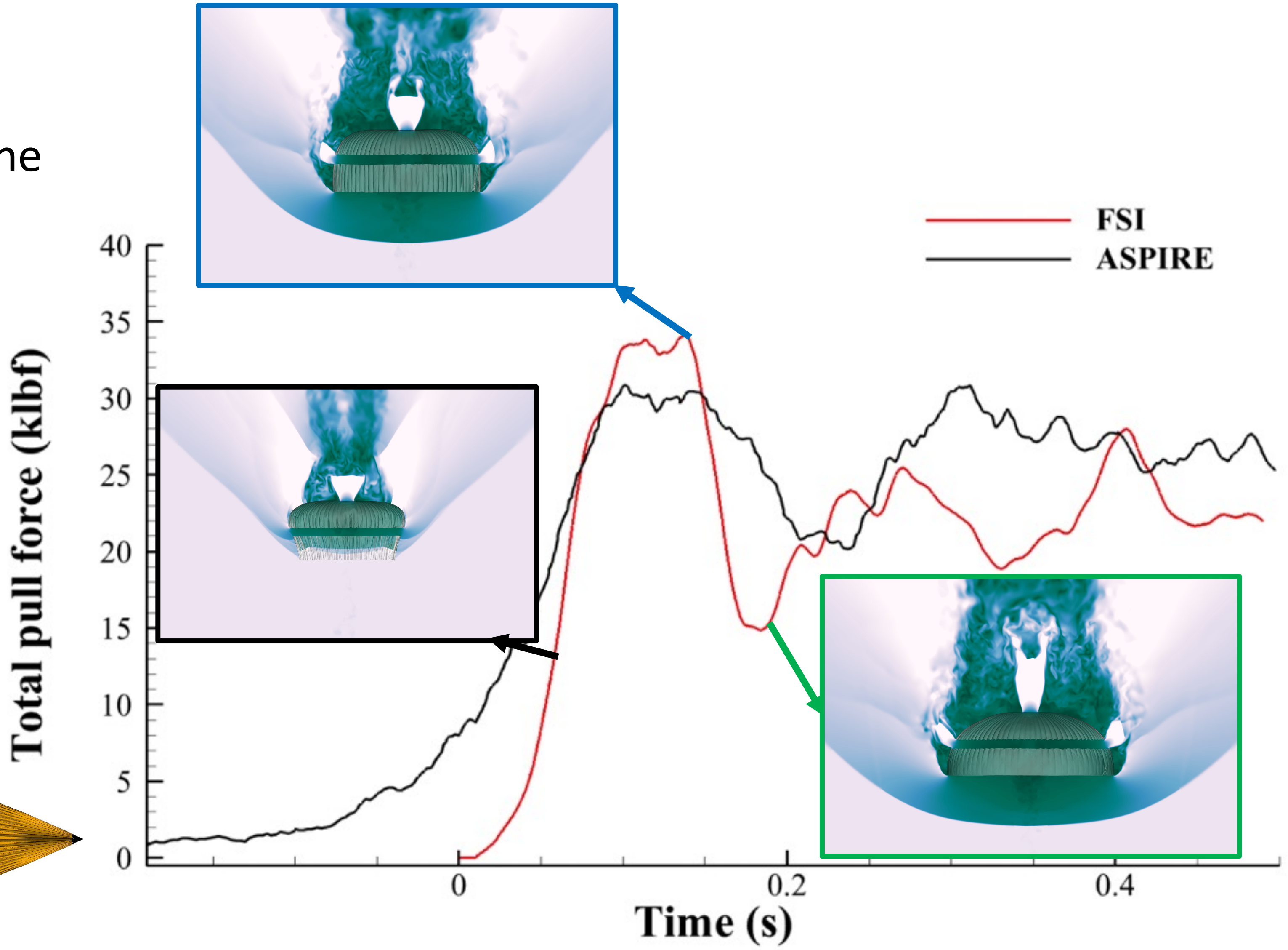

Grid Resolution Study: ASPIRE FSI

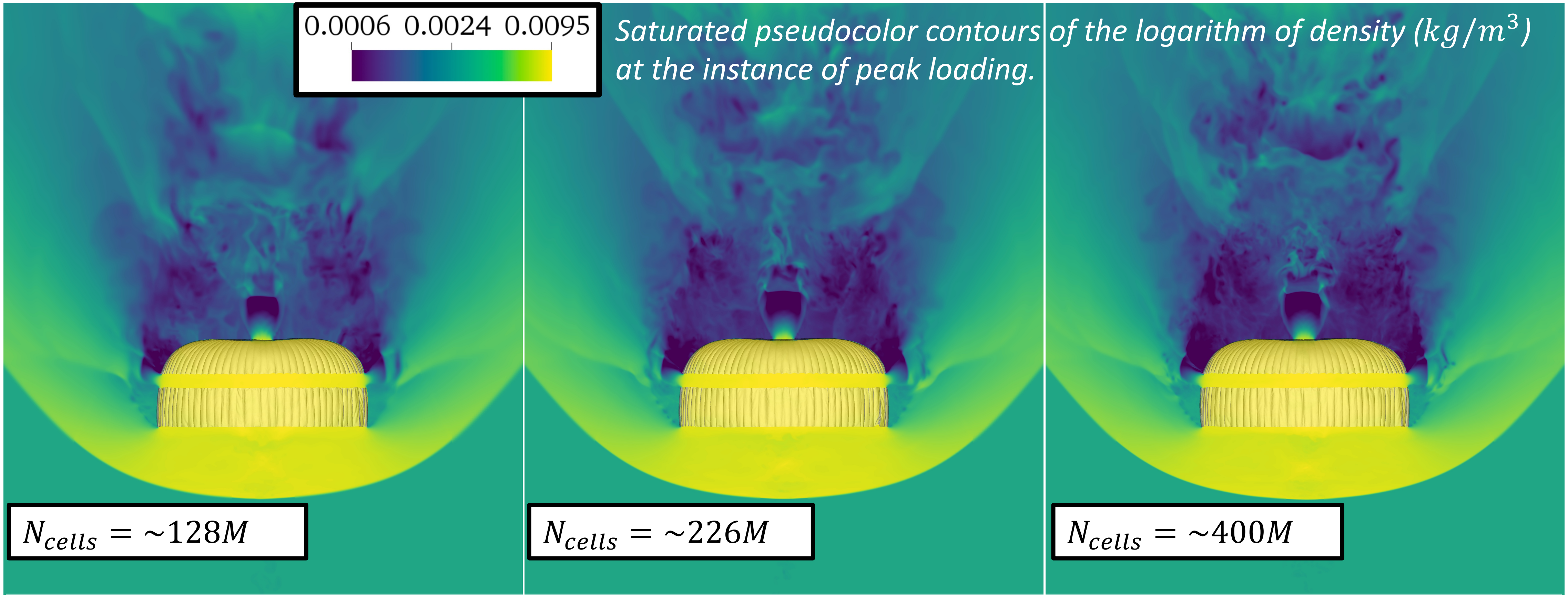

- Qualitatively, the primary flow features are very similar between grids
  - The wake width, bow shock shape, and wake recompression shock are all very similar
  - The primary differences lie in the resolution of smaller scale flow features that do not seem to affect the aerodynamic drag significantly

Grid Resolution Study: ASPIRE FSI

- ❑ All three volume resolutions predict peak loads within 1% of each other

- ❑ ~9% difference in the peak load predicted by the simulation and that from flight test data
  - 3.3% uncertainty in flight data at peak load

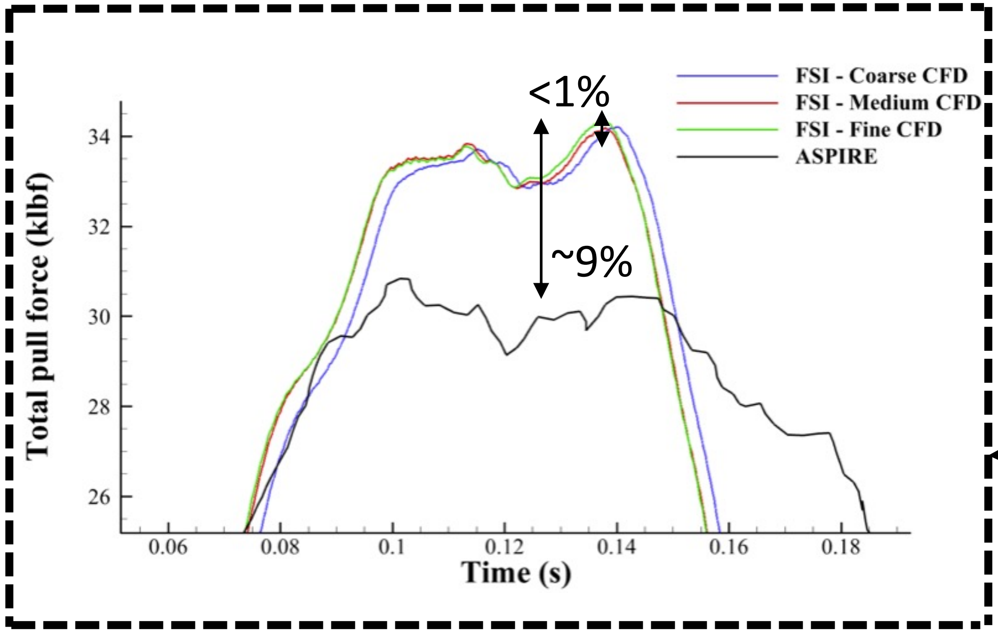

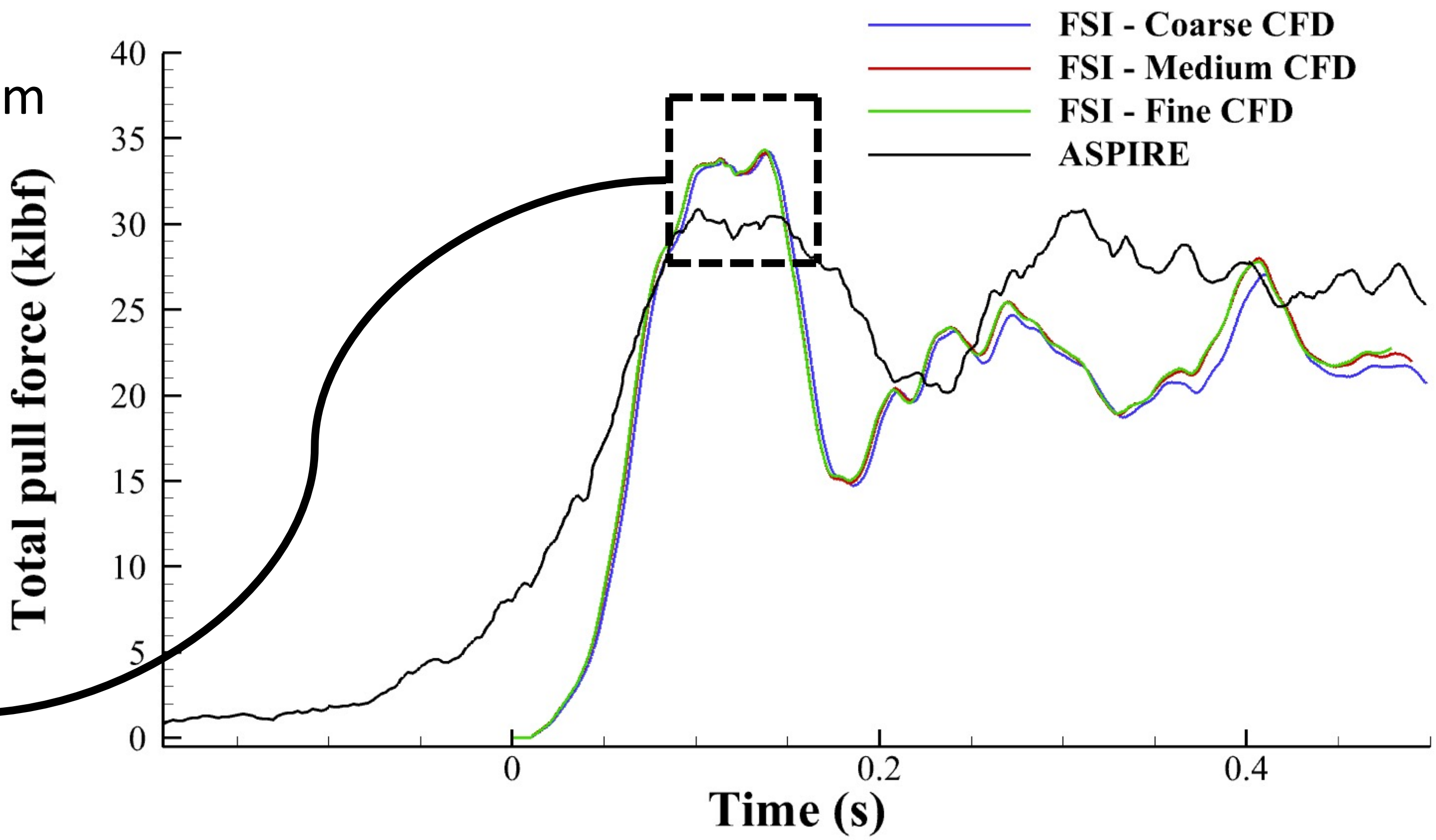

Grid Resolution Study: ASPIRE FSI

- The coarse and medium grid solutions are projected onto the fine grid signal
  - Compute the absolute differences in the solutions
  - Convergent behavior is evident

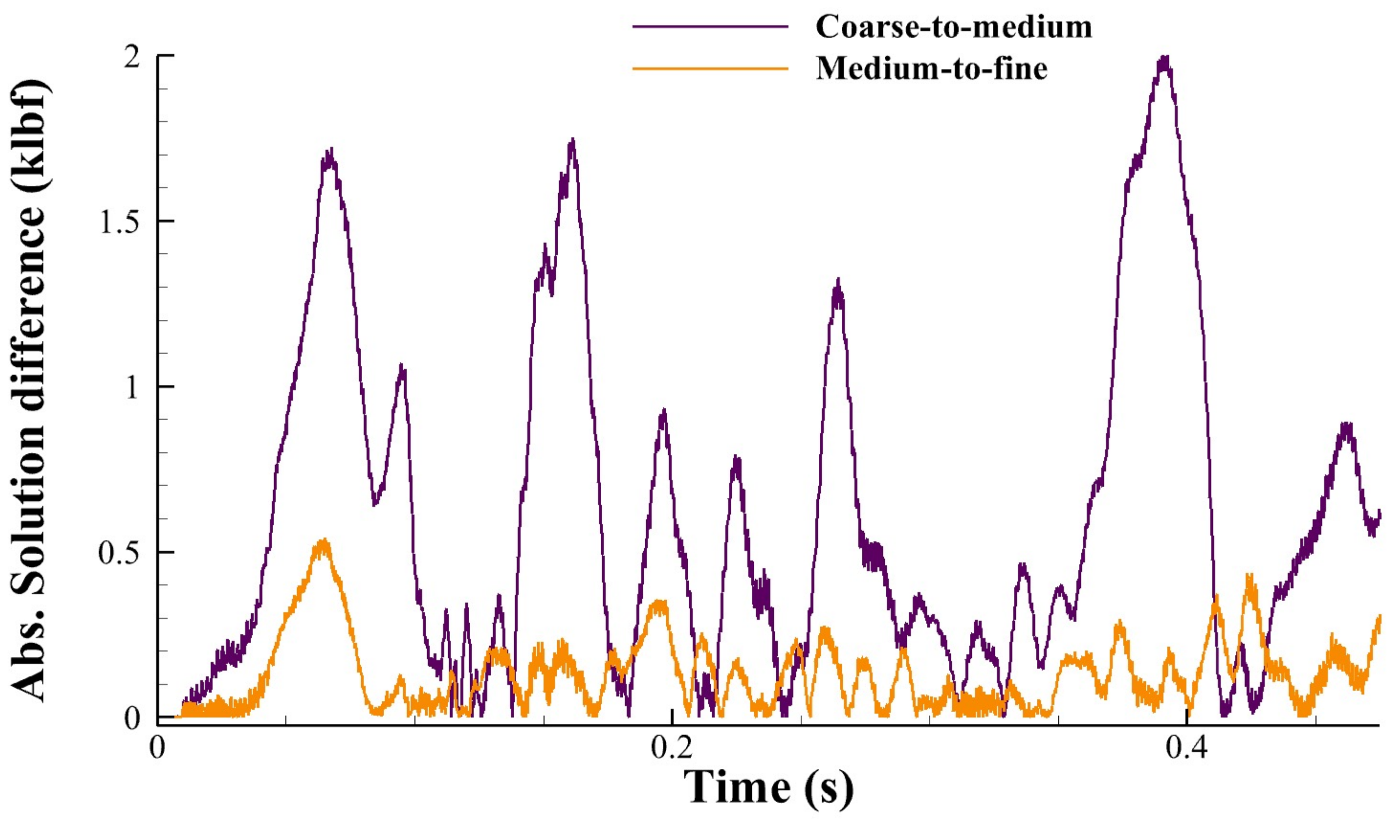

Grid Resolution Study: ASPIRE FSI

- The coarse and medium grid solutions are projected onto the fine grid signal
  - Compute the absolute differences in the solutions
  - Convergent behavior is evident

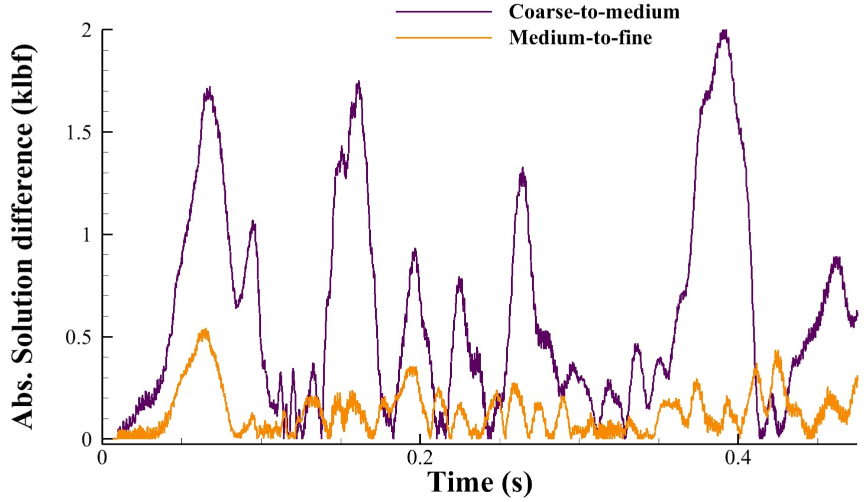

- An attempt is made to quantify the uncertainty
  - The “inflation interval” of [0.095s, 0.145s] is considered

- Less than 0.15% grid-related uncertainty for both metrics

Metric	Coarse	Medium	Fine	GCI	Est. Converged Value	Est. Uncertainty
Peak Load (klbf)	33.2653	33.3620	33.3979	0.0014856	33.4255	±0.047142
Peak Impulse (klbf·s)	1.6629	1.6679	1.6696	0.0013108	1.6707	±0.002190

- Convergence rate of ~4 is computed, but likely does not reflect order of numerical method
  - However, implies temporal discretization error is small compared to spatial discretization error

Structural Grid Refinement: ASPIRE FSI

- ❑ The structural mesh is refined such that the average edge length is a factor $2^{\frac{1}{3}}$ smaller than the base mesh
- ❑ Again, the solution displays very little sensitivity to increasing resolution

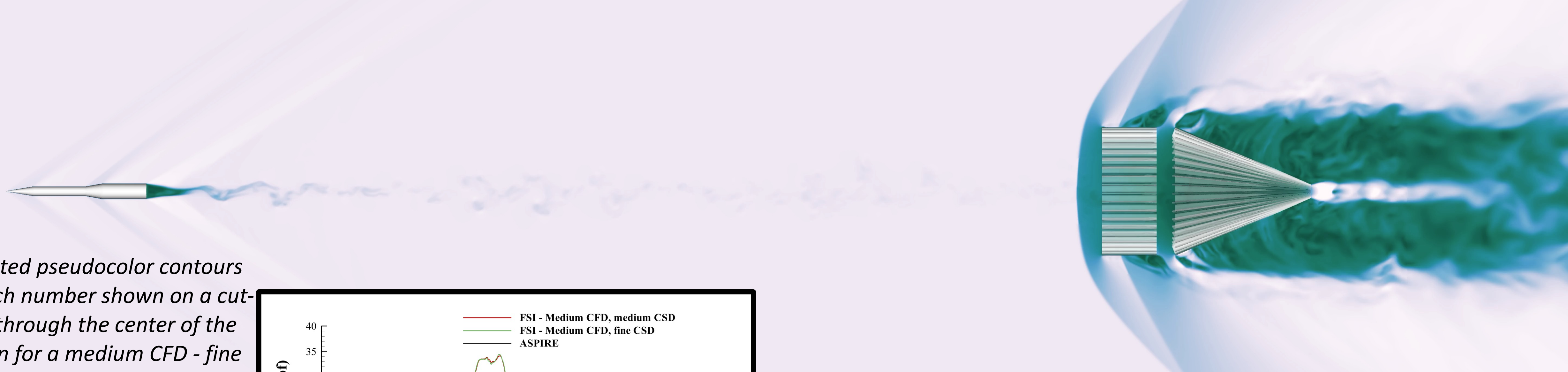

Saturated pseudocolor contours of Mach number shown on a cut-plane through the center of the domain for a medium CFD - fine CSD simulation of ASPIRE SR01.

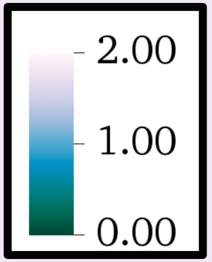

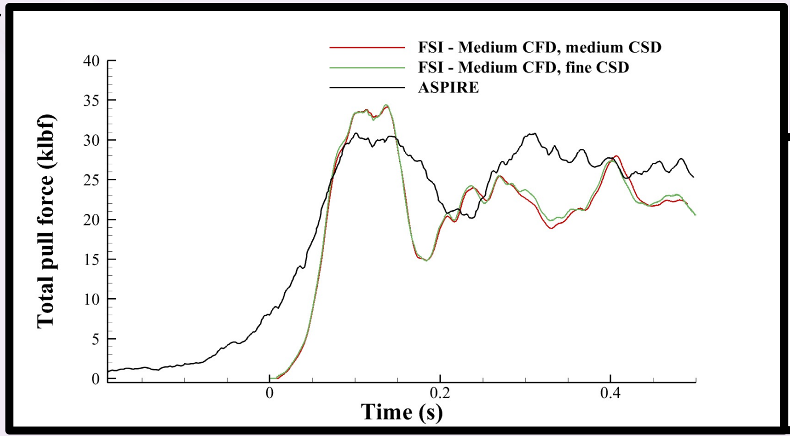

Simulation	N_{cores}	Duration (hours)	Resources (core-hours)
Coar. CFD - Med. CSD	1600	32	51,200
Med. CFD - Med. CSD	960	67	64,320
Fine CFD - Med. CSD	2400	70	168,000
Med. CFD - Fine CSD	2400	58	139,200

Summary

- A capability to simulate supersonic parachute inflation has been demonstrated

- Methods to model broadcloth porosity and contact mechanics were developed and validated

- The LAVA-Cartesian/Structural FSI capability was validated using ASPIRE flight data
  - LAVA FSI simulations predict peak loading within ~9% of that measured during the flight test
  - Grid convergence with respect to the volume domain resolution was demonstrated for FSI simulations
  - The solution sensitivity with respect to the surface/structural resolution was studied
  - The remaining modeling error between the simulations and flight is attributed to other factors not yet considered

- Next steps include investigating modeling deficiencies, *e.g.*, initial fluid-structural state/topology, inelastic and orthotropic material modeling, and capsule deceleration

A special thanks to ESM for providing the opportunity to work on this challenging problem